Nuclear Spin-Lattice Relaxation in the One-Dimensional Ferrimagnet $Mn(hfac)_2NITiPr$

Fabrizio Ferraro,[†] Dante Gatteschi,*[,†] Roberta Sessoli,[†] and Maurizio Corti[‡]

Contribution from the Department of Chemistry, University of Florence, Florence, Italy, and Department of Physics "A. Volta", Unita' GNSM-INFM and Sezione INFN, University of Pavia, Pavia, Italy. *Received February 20, 1991*

Abstract: $Mn(hfac)_2(NITiPr)$, where hfac is hexafluoroacetylacetonate and NITiPr is 2-isopropyl-4,4,5,5-tetramethyl-4,5-dihydro-1*H*-imidazoline-1-oxyl 3-oxide, is a one-dimensional ferrimagnet that orders ferromagnetically at ca. 8 K. NMR experiments performed on polycrystalline powders and single crystals in the paramagnetic phase show that the spin-lattice relaxation rates of both ^1H and ^{19}F in the range 8-90 MHz follow a $\nu^{-1/2}$ dependence down to about 20 MHz, while below the frequency dependence is reversed. The frequency dependence above 20 MHz is typical of a one-dimensional magnetic material, confirming that ferrimagnets are similar to ferromagnets and antiferromagnets under this respect. The breakdown of $\nu^{-1/2}$ dependence observed in the low-frequency range is related to a cutoff mechanism of spin-diffusive behavior, due to intrachain dipolar interactions. This result sets an upper limit to the interchain exchange coupling $J' \leq 6 \times 10^{-4}$ cm^{-1}, which confirms the dipolar model for magnetic ordering previously suggested.

Introduction

Magnetic molecular materials exhibiting spontaneous magnetization below a critical temperature are attracting increasing interest.[1-10] Although the critical temperatures to three-dimensional magnetic order are still closer to the liquid helium than to the liquid nitrogen range, the reported materials have already shown new magnetic behaviors, which provide useful testing grounds for existing theories or good opportunities for extending them.

Essentially all the magnetic molecular materials reported so far order three-dimensionally starting from one-dimensional structures so that, in order to understand which are the driving forces to magnetic order, it is necessary to have a good understanding of the high-temperature low-dimensional properties.[11-17]

Magnetic resonance techniques are extremely well suited to characterize one-dimensional materials,[18-22] showing peculiar features that provide information on the spin dynamics,[23-28] on the structural properties, and on the phase transitions.[29,30] Magnetic resonance studies have initially concentrated on the one-dimensional ferromagnets and antiferromagnets, because initially these were the only types of materials available.

The recently reported one-dimensional ferrimagnets[31-35] have opened new possibilities of investigation. EPR, which is well known to provide a very powerful tool in order to obtain a deep insight into the properties of these materials,[35-39] showed that the one-dimensional ferrimagnet, which up to now conforms better to the ideal behavior, is $Mn(hfac)_2(NITiPr)$,[35-40] where hfac = hexafluoroacetylacetonato and NITiPr = 2-isopropyl-4,4,5,5-tetramethyl-4,5-dihydro-1*H*-imidazoline-1-oxyl 3-oxide, whose structure is reported in Figure 1.[35] In fact, EPR spectra provided an upper limit to the inter- to intrachain exchange ratio J'/J of 10^{-3} and the preferred spin orientation in the paramagnetic phase, which suggested that the driving force to three-dimensional magnetic order for this compound is the dipolar interaction between the chains. Although this interpretation seems reasonable, there is still some possibility of doubt, because with $J = 330$ cm^{-1}, estimated from the magnetic susceptibility, the upper limit of $J \cong 0.3$ cm^{-1} would still allow an exchange-determined magnetic order.

In order to have a direct measurement of weak interactions, NMR is intrinsically better suited than EPR, because it samples the response of the systems to the low-frequency magnetic excitations. Therefore, we decided to record the NMR spectra and measure the relaxation times of ^1H and ^{19}F in $Mn(hfac)_2(NITiPr)$ in order to check whether they can indeed provide a direct measurement of the interchain interactions, and consequently precious information on the mechanism of magnetic order in this class of magnetic molecular materials. We report here the results of this investigation, together with the development of the necessary

[†] University of Florence.
[‡] University of Pavia.

(1) Gatteschi, D., Kahn, O., Miller, J. S., Palacio, F., Eds. *Magnetic Molecular Materials*; NATO ASI Series E198; Kluwer: Dordrecht, 1991.
(2) Miller, J. S.; Epstein, A. J.; Reiff, W. R. *Acc. Chem. Res.* **1988**, *21*, 14.
(3) Kahn, O. *Angew. Chem., Int. Ed. Engl.* **1985**, *24*, 834.
(4) Iwamura, H. *Pure Appl. Chem.* **1987**, *59*, 1585.
(5) Caneschi, A.; Gatteschi, D.; Sessoli, R.; Rey, P. *Acc. Chem. Res.* **1989**, *22*, 392.
(6) Dougherty, D. A. *Mol. Cryst. Liq. Cryst.* **1989**, *176*, 25.
(7) Broderick, W. E.; Thompson, J. A.; Day, E. P.; Hoffman, B. M. *Science* **1990**, *249*, 401.
(8) Breslow, R. *Pure Appl. Chem.* **1982**, *54*, 927.
(9) Dorman, E.; Nowak, M. J.; Williams, K. A.; Angus, R. O., Jr.; Wudl, F. J. *J. Am. Chem. Soc.* **1987**, *109*, 2594.
(10) Coronado, E.; Drillon, M.; Nutgeren, P. R.; de Jongh, L. J.; Beltran, D.; Georges, R. *J. Am. Chem. Soc.* **1989**, *111*, 3874.
(11) Renard, J.-P. In *Organic and Inorganic Low-Dimensional Crystalline Materials*; Delhaes, P., Drillon, M., Eds.; NATO ASI Series B168; Plenum Press: New York, 1987; p 125.
(12) Landee, C. P. In *Organic and Inorganic Low-Dimensional Crystalline Materials*; Delhaes, P., Drillon, M., Eds.; NATO ASI Series B168; Plenum Press: New York, 1987; p 75.
(13) de Jongh, L. J. In *Magneto-Structural Correlations in Exchange Coupled Systems*; Willett, R. D., Gatteschi, D., Kahn, O., Eds.; NATO ASI Series C140; Reidel: Dordrecht, 1985; p 1.
(14) Bonner, J. C. In *Magneto-Structural Correlations in Exchange Coupled Systems*; Willett, R. D., Gatteschi, D., Kahn, O., Eds.; NATO ASI Series C140; Reidel: Dordrecht, 1985; p 157.
(15) Willett, R. D.; Gaura, R. M.; Landee, C. P. In *Extended Linear Chain Compounds*; Miller, J. S., Ed.; Plenum Press: New York, 1983; p 143.
(16) Bray, J. W.; Interrante, L. V.; Jacobs, I. S.; Bonner, J. C. In *Extended Linear Chain Compounds*; Miller, J. S., Ed.; Plenum Press: New York, 1983; p 353.
(17) Hatfield, W. E.; Estes, W. E.; Marsh, W. E.; Pickens, M. W.; ter Haar, L. W.; Weller, R. R. In *Extended Linear Chain Compounds*; Miller, J. S., Ed.; Plenum Press: New York, 1983; p 43.
(18) Drumheller, J. E. *Magn. Reson. Rev.* **1982**, *7*, 123.
(19) Richards, P. M. In *Local Properties at Phase Transitions*; Muller, K. A., Rigamonti, A., Eds.; Editrice Compositori: Bologna, 1976; p 359.
(20) Gatteschi, D.; Sessoli, R. *Magn. Reson. Rev.* **1990**, *15*, 1.
(21) Renard, J.-P. In *Magneto-Structural Correlations in Exchange Coupled Systems*; Willett, R. D., Gatteschi, D., Kahn, O., Eds.; NATO ASI Series C140, Reidel: Dordrecht, 1985; p 207.
(22) Soos, Z. G.; Bondeson, S. R. In *Extended Linear Chain Compounds*; Miller, J. S., Ed.; Plenum Press: New York, 1983; p 193.
(23) Borsa, F.; Mali, M. *Phys. Rev.* **1974**, *B9*, 2215.
(24) Boucher, J.-P.; Ahmed Bakheit, M.; Nechtschein, M.; Villa, M.; Bonera, G.; Borsa, F. *Phys. Rev.* **1976**, *B13*, 4098.
(25) Hone, D.; Scherer, C.; Borsa, F. *Phys. Rev.* **1974**, *B9*, 965.
(26) Boucher, J.-P.; Renard, J.-P. *Phys. Rev. Lett.* **1980**, *45*, 486.
(27) Jeandey, C.; Boucher, J.-P.; Ferrieu, F.; Nechtschein, M. *Solid State Commun.* **1977**, *23*, 673.
(28) Clement, S.; Veillet, P.; Cheikh-Rouhou, A. *J. Phys.* **1987**, *C20*, 5187.

0002-7863/91/1513-8410$02.50/0

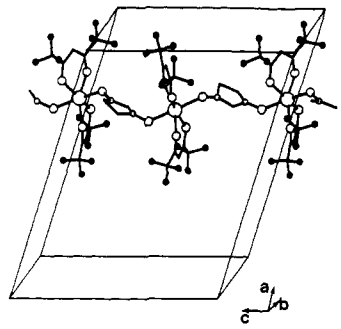

Figure 1. View of the chain structure of $Mn(hfac)_2(NITiPr)$. The fluorine atoms are represented by filled circles while methyl groups and hydrogen atoms are not reported for sake of clarity.

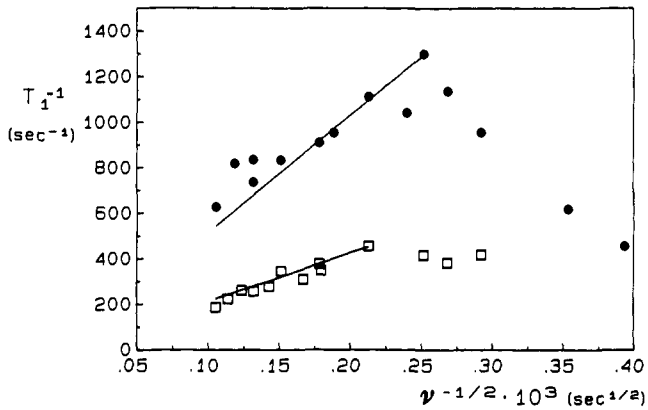

Figure 2. ^1H (●) and ^{19}F (□) spin-lattice relaxation rates of polycrystalline powders of $Mn(hfac)_2(NITiPr)$ at various frequencies. The lines are best fit curves calculated as described in the text.

theoretical framework, and hope to be able to show how indeed NMR experiments can provide a deep insight into the magnetic properties and spin dynamics of molecular magnetic materials.

Experimental Section

$Mn(hfac)_2(NITiPr)$ single crystals were obtained as previously described.[35] They are long thin shaped with elongation axes corresponding to the *c* crystallographic axes, along which the chains are directed.

NMR measurements were performed on a pulse FT spectrometer, built around a pulse programmer, a double-side band rf switch, and a receiver by MMid-Continent Instrument, an ENI LPI-10 wide-band power amplifier, and a Fluke 6060A synthesized rf generator. The acquisition and the digital manipulation of the NMR FID signals was performed by an HP 54501A digitizer interfaced to an Olivetti M24-pc, while the static magnetic field was generated by a Bruker B-M-10 electromagnet.

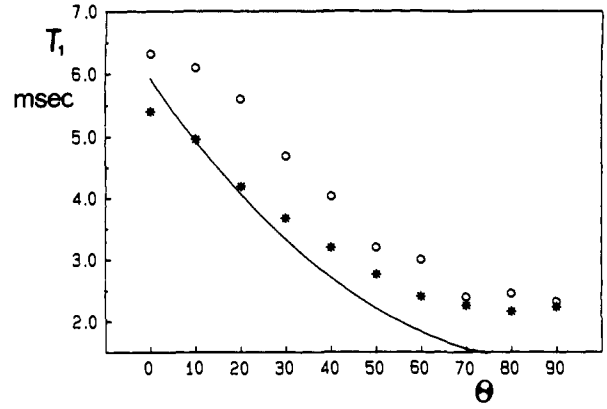

Figure 3. Angular dependence of the ^{19}F spin-lattice relaxation time of single crystals of $Mn(hfac)_2(NITiPr)$ at 65 MHz (○) and 48 MHz (*), respectively. θ is the angle of the external magnetic field with the chain axis. The line is the curve calculated as described in the text at 65 MHz.

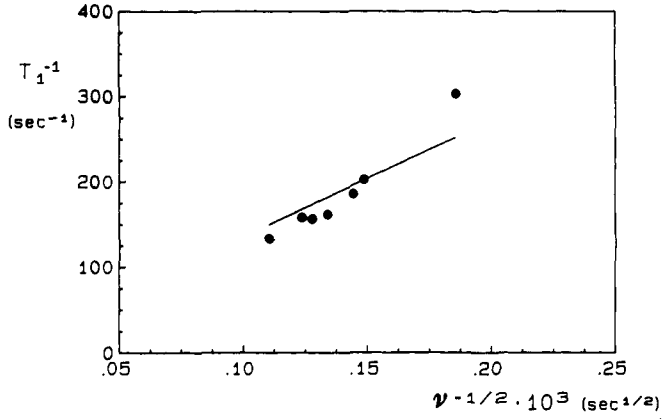

Figure 4. ^{19}F spin-lattice relaxation rates of single crystals of $Mn(hfac)_2(NITiPr)$ with the external magnetic field parallel to the chain axis. The line is the best fit curve calculated with (7).

^1H and ^{19}F resonance spectra, T_1, and T_2 on the powdered sample at various frequency in the range 8–90 MHz were recorded. Oriented crystals ^{19}F T_1 were obtained in the frequency range 29–82 MHz at various orientations of the crystals with respect to the external magnetic field.

Results

The NMR spectra of polycrystalline powders of $Mn(hfac)_2(NITiPr)$ in the frequency range 11–90 MHz show a single line for both ^{19}F and ^1H nuclei, about 30 and 65 KHz wide, respectively. The ^1H spectrum at high frequency (90 MHz) is an exception, showing two shoulders flanking the central line at about ±25 KHz. Line shape analysis of the free induction decay, FID, indicates that the observed lines are approximately Gaussian.

Spin-lattice relaxation times, T_1, were obtained by using the standard saturation recovery method characterized by the pulse sequence $(90°-\tau-90°-AQ-DT)_n$. The recovery of the longitudinal equilibrium magnetization after the first $\pi/2$ pulse is analyzed by applying the reading pulse after a variable delay τ and by following the values assumed by the FID after a fixed time t.

In the powdered samples, the recovery was found to be monoexponential over one decade. The relaxation rates for the two nuclei are plotted in Figure 2 versus $\nu_n^{-1/2}$. It is apparent that at high frequencies the relaxation rates of both nuclei yield a reasonably linear dependence, increasing with increasing $\nu_n^{-1/2}$, but below $\nu_n \cong 17$ and 22 MHz for ^1H and ^{19}F, respectively, the experimental relaxation rates decrease with decreasing frequency.

Single crystals of $Mn(hfac)_2(NITiPr)$ were not big enough to allow a direct NMR measurement, due to sensitivity reasons. However, it was possible to use a bunch of isooriented crystals on a suitable sample holder. The habitus of the crystals is that of needles with the elongation axis corresponding to the chain axis, so that it was relatively easy to orient them all with parallel long

(29) Dupas, C.; Renard, J.-P. *Solid State Commun.* **1976**, *20*, 581. Dupas, C.; Renard, J.-P. *Phys. Lett.* **1973**, *43A*, 119. Magnum, B. W.; Utton, D. B. *Phys. Rev.* **1972**, *B6*, 2790.
(30) Borsa, F.; Boucher, J.-P.; Villain, J. *J. Appl. Phys.* **1978**, *49*, 1326.
(31) Gleizes, A.; Verdaguer, M. *J. Am. Chem. Soc.* **1984**, *106*, 3727.
(32) Pei, Y.; Verdaguer, M.; Kahn, O.; Sletten, J.; Renard, J.-P. *J. Am. Chem. Soc.* **1986**, *108*, 7428.
(33) Landee, C. P.; Djili, A.; Mudgett, D. F.; Newhall, M.; Place, H.; Scott, B.; Willett, R. D. *Inorg. Chem.* **1988**, *27*, 620.
(34) Coronado, E.; Drillon, M.; Fuertes, A.; Beltran, D.; Mosset, A.; Galy, J. *J. Am. Chem. Soc.* **1986**, *108*, 900.
(35) Caneschi, A.; Gatteschi, D.; Rey, P.; Sessoli, R. *Inorg. Chem.* **1988**, *27*, 1756.
(36) Gatteschi, D.; Guillou, O.; Zanchini, C.; Sessoli, R.; Kahn, O.; Verdaguer, M.; Pei, Y. *Inorg. Chem.* **1989**, *28*, 287.
(37) Gatteschi, D.; Sessoli, R.; Zanchini, C. In *Magnetic Resonance and Related Phenomena*, Proceedings of the 24th Ampere Conference, Poznan, 1988; Stankoski, J., Pislewski, N., Hoffmann, S. K., Idziak, S., Eds.; Elsevier: Amsterdam, 1989; p 325.
(38) Caneschi, A.; Gatteschi, D.; Renard, J.-P.; Rey, P.; Sessoli, R. *Inorg. Chem.* **1989**, *28*, 3314.
(39) Gatteschi, D.; Zanchini, C.; Kahn, O.; Pei, Y. *Chem. Phys. Lett.* **1989**, *160*, 157.
(40) Caneschi, A.; Gatteschi, D.; Reynard, J.-P.; Rey, P.; Sessoli, R. *Inorg. Chem.* **1989**, *28*, 1976.

axes. Since the four developed (100), (010), ($\bar{1}$00), and (0$\bar{1}$0) faces cannot be morphologically recognized, the crystals were randomly glued to the sample holder lying on these faces. As a consequence, the external field has a random projection on the *ab* plane.

The longitudinal magnetization recovery was found to be described by a single exponential for θ angles smaller than 50°, where θ is the angle between the external magnetic field and the chain axis. For larger angles, we observe some deviations from monoexponential at the end of the first decade, but so small that we cannot properly define either a biexponential recovery or a distribution of T_1's: In these cases, the T_1 value is the one better reproducing the recovery as a monoexponential decay.

The spin–lattice relaxation times of ^{19}F measured on oriented crystals are plotted in Figure 3 as a function of θ at two frequencies. The plots show a monotonic decrease of T_1 on increasing θ. The angular variation of the relaxation time is remarkable and more evident at the higher frequencies. The frequency dependence of the spin–lattice relaxation rates of ^{19}F in the range 29–82 MHz for $\theta = 0°$ is plotted in Figure 4. In this range, the spin–lattice relaxation rate is linear with $\nu_n^{-1/2}$.

Spin–spin relaxation times, T_2, were measured by using the standard technique of the Hahn spin-echo method defined by the pulse sequence $(90_x°-\tau-180_y°-\tau-\text{AQ}-\text{DT})_n$, which permits the refocusing of the transversal components of the magnetization after the time 2τ.

The measured T_2 was found to be much shorter than T_1 at various frequencies. It is ca. 30–40 μs for both ^{1}H and ^{19}F in the powders, and about 70–80 μs for ^{19}F in the oriented crystal sample. Noteworthy is that the T_2's are longer than the corresponding T_2^*'s, which describe the FID and determine the line width (for the powders, $T_2 \cong 30$–40 μs versus $T_2^* \cong 5$ μs; for the oriented crystals, (i) with $\theta = 0°$, $T_2 \cong 70$ μs versus $T_2^* \cong 30$ μs, (ii) with $\theta = 90°$, $T_2 \cong 80$ μs versus $T_2^* \cong 13$ μs).

Discussion

Theoretical Model. In a one-dimensional magnetic solid, the relaxation rate of a $I = {}^1/_2$ nucleus, which might be either ^{1}H or ^{19}F, is determined by the fluctuations of the field at the nuclear site due to the electron spins.[41,42] The homonuclear dipolar contribution to the relaxation is negligible due to the lower intensity of the interactions compared to the nuclei–electrons ones, and because the nuclear motions are much slower than the motions of the electrons. In the high-temperature limit ($kT \gg JS(S+1)$ for a chain of spins), where the electron spins are largely uncorrelated, the magnetic field felt by the nucleus is the sum of the contributions of the dipolar and isotropic components of all the electron spins in the lattice:

$$\mathbf{h} = \sum_i \mathbf{h}_i = -\sum_i \gamma_e \hbar \left[\frac{\mathbf{S}_i}{r_i^3} - \frac{3(\mathbf{r}_i \mathbf{S}_i)\mathbf{r}_i}{r_i^5} \right] + \frac{A_i}{\gamma_e} \mathbf{S}_i \qquad (1)$$

where i numerates the spins in the lattice, r_i is the distance of the nucleus from the electron spin, and A_i is the corresponding constant for the contact interaction. Pseudocontact interactions can be safely neglected in this case, when the electron spins are highly isotropic.

The spin–lattice relaxation rate can be written as[24,28]

$$T_1^{-1} = {}^2/_3 S(S+1)\gamma_e^2 \gamma_n^2 \hbar^2 \sum_{ij} [a_{ij}^z j_{ij}^z(\omega_n) + a_{ij}^+ j_{ij}^+(\omega_e)] \qquad (2)$$

where the a_{ij}^α's are numerical coefficients that can be calculated by using the dipolar and contact components of (1) and the spectral density $j_{ij}^\alpha(\omega)$ are the Fourier transforms of the correlation functions of the spin components:

$$j_{ij}^\alpha(\omega) = \int g_{ij}^\alpha(t) \exp(i\omega t)\, dt \qquad (3)$$

$$g_{ij}^\alpha(t) = \langle S_i^\alpha(0) S_j^{\alpha *}(t) \rangle \qquad (4)$$

with i and j numerating two spin centers. The physical meaning of the correlation function is that of providing information on how a system on which a perturbation is created at time $t = 0$ reverts to thermal equilibrium. $\langle S_i^\alpha(0) S_j^{\alpha *}(t) \rangle$ is a statement of the probability that the perturbation created on site i is located on site j at time t. If the system does not react to the perturbation, the normalized correlation function is equal to zero and independent of time.

On the NMR time scale, the most important mechanism that allows the system to return to equilibrium is spin diffusion,[43] caused by the gradient of magnetization generated by the perturbation. This mechanism strongly depends on the type of system. In fact, the correlation decays as $t^{-d/2}$, where d is the lattice dimensionality.[19] For three-dimensional systems, the $t^{-3/2}$ dependence is so fast that the effects of the spin diffusion do not show up in the spectra. Conversely the $t^{-1/2}$ dependence for one-dimensional materials determines a very slow decay of the spin correlation because exchange is much less effective in one dimension than in three dimensions to keep the spins informed of what is happening in the lattice. It is therefore the persistence of the correlation that gives unique features to the magnetic resonance spectra and relaxation times of one-dimensional magnetic materials.

The diffusive behavior is given, for one-dimensional systems, by[44,45]

$$g_{ij}(t) = (4\pi D t)^{-1/2} \exp[-(i-j)^2/4Dt] \qquad (5)$$

D is a parameter related to the efficiency of spin diffusion, which both calculations[46,47] and experiments[24] showed to be of the order of $\omega_{ex} \approx J/\hbar$. At long times, all the spin correlation functions become equivalent, because the exponential tends to 1. The corresponding spectral densities, and the spin–lattice relaxation rates, depend on $\omega^{-1/2}$ in the high-temperature limit.[23] Therefore, a linear frequency dependence of T_1^{-1} on $\omega^{-1/2}$ is an indication of one-dimensional behavior.

Deviations of the relaxation rates from diffusive behavior can be observed at long times (corresponding to small NMR frequencies) as the result of either interchain interactions, which effectively transform the system in a two- or three-dimensional material, or also by intrachain dipolar interactions when they have a frequency comparable to the nuclear Larmor frequency. Both effects can be described by a fast decay of the correlation function, which goes rapidly to zero around a cutoff time t_c. The corresponding cutoff frequency, ω_c, can be determined in a variable-frequency experiment as the frequency at which the diffusive behavior is lost. Therefore, the determination of the frequency dependence of the nuclear spin–lattice relaxation rate is a very sensitive way of determining how effectively one-dimensional a material really is, and also to give an insight into the reasons that make it deviate from diffusive behavior.[23,24,27]

Calculations. In order to calculate the relaxation rates with (2), it is necessary to have a knowledge both of the electron–nucleus coupling coefficients and of the diffusion coefficients or simply of the exchange frequency.

The theoretical approach extensively reported in ref 24 and the development of ref 27 need some changes in order to apply (2) to the one-dimensional ferrimagnet Mn(hfac)(NITiPr). First of all, the crystal structure[35] shows the existence of 24 and 26 magnetically different fluorine and hydrogen atoms, respectively. In fact, although the asymmetric unit in the cell comprises 12 fluorine and 13 hydrogen atoms, the chain structure is obtained by the application of the glide plane, which makes adjacent units magnetically not equivalent.

Each fluorine and hydrogen atom should relax according to its own T_1, and as a result the observed recovery of the equilibrium magnetization should be polyexponential also in a single crystal.

(41) Dingle, R.; Lines, M. E.; Holt, S. L. *Phys. Rev.* **1969**, *187*, 643.
(42) Hutchings, M. T.; Shirane, G.; Birgenau, R. J.; Holt, S. L. *Phys. Rev. B* **1972**, *5*, 1999.
(43) Kadanoff, L.; Martin, P. C. *Ann. Phys. (N.Y.)* **1963**, *24*, 419. Bennett, H. S.; Martin, P. C. *Phys. Rev.* **1965**, *A138*, 608.
(44) Blume, M.; Hubbard, J. *Phys. Rev.* **1970**, *B1*, 3815.
(45) McLean, F. B.; Blume, M. *Phys. Rev.* **1973**, *B7*, 1149.
(46) Lurie, N. A.; Huber, D. L.; Blume, N. *Phys. Rev.* **1974**, *B9*, 2171.
(47) Carboni, F.; Richards, P. M. *Phys. Rev.* **1969**, *177*, 889.

Experimentally we always observe a monoexponential process, except in the oriented crystal data in which, for $\theta > 50°$, there are some deviations that however are not large enough to define the parameters for multiexponential decay.

The observation of a single T_1 is probably due to the short values of T_2, which cause the occurrence of one common spin temperature for ^1H and another for ^{19}F. As a consequence, the equation (2) for T_1^{-1} must be modified to take into account that the experimental relaxation rate is the average of the individual relaxation rates of the various nuclei. A similar procedure was previously used in the interpretation of the NMR data of the one-dimensional ferromagnet CHAC.[28]

We assume that the dipolar contributions are dominant in the electron–nucleus coupling on the basis of the following considerations: (i) the contact contribution must be small because the nuclei and the electron sites are separated by at least three σ bonds;[48] (ii) the strong angular dependence of the experimental relaxation rate which shows that in every case the main contribution is dipolar in origin.

Different from the previously reported cases of one-dimensional ferromagnets[28] or antiferromagnets,[23] we must consider that here the relaxation is due to the interaction with both the $S = {}^5/_2$ spins of manganese(II) and the $S = {}^1/_2$ spins of the radicals. Actually, since we must compute the two-spin correlation functions, we have to deal with correlation functions of two Mn spins, of two radical spins, and of the cross correlation of a Mn and a radical spin. The corresponding dipolar coefficients are expected to scale as

$$S_{Mn}(S_{Mn} + 1)/r_{NMn}{}^6 : \sqrt{S_{Mn}(S_{Mn} + 1)S_R(S_R + 1)}\Big/ (r_{NMn}{}^3 r_{NR}{}^3) : S_R(S_R + 1)/r_{NR}{}^6 \quad (6)$$

where N indicates a nucleus and R a radical and r is the distance between the indicated centers. The delocalized radical spin can be considered to be placed with half an electron on each NO group.[49]

For hydrogen atoms, the three contributions are comparable, and no one can be neglected in the calculation. For fluorine nuclei on the other hand, the most important contribution comes from the interaction with the Mn centers, thus simplifying the calculations.

Taking into account that at long times all the correlation functions become equal, the spin–lattice relaxation rate for the fluorine nuclei can be expressed as

$$T_1^{-1} = {}^2/_3\beta^2 S_{Mn}(S_{Mn} + 1)\chi(0)\{A^z j^z(\omega_N) + A^+ j^+(\omega_e)\} \quad (7)$$

$A^\alpha = \sum_p A_p/N = \alpha^2 \sum_p \sum_l \sum_j \sum_l a^\alpha_{i,p,l} a^\alpha_{i+j,p,l}/N$ and $\beta^2 = \gamma_e{}^2 \gamma_n{}^2 \hbar^2$, with p numerating the various nuclei and l the different nearest chains and the a^α coefficients being the nuclei–electrons dipolar coupling coefficients expressed as functions of the radial coordinates $r_{i,p}$, $\theta_{i,p}$, and $\varphi_{i,p}$, with the azimuthal axis coincident with the chain axis:

$$a^z_{ij} = {}^9/_4(\sin\theta_i \cos\theta_i \sin\theta_j \cos\theta_j) \cos(\varphi_i - \varphi_j)/(r_i{}^3 r_j{}^3) \quad (8)$$

$$a^+_{ij} = {}^1/_8\{(1 - 3\cos^2\theta_i) \times (1 - 3\cos^2\theta_j) + 9\sin^2\theta_i \sin^2\theta_j \cos 2(\varphi_i - \varphi_j)\}/(r_i{}^3 r_j{}^3) \quad (9)$$

$\chi(0)$ is the static susceptibility, which must be taken into account because in $Mn(hfac)_2(NITiPr)$ the high-temperature limit is not attained due to the large intrachain coupling constant. The spectral density functions $j^z(\omega)$ and $j^+(\omega)$ are equal to each other at high temperature due to the isotropy of the exchange Hamiltonian.

In the actual calculation, we have considered the interaction of the fluorine nuclei with the 20 nearest neighbor chains, each made of 30 manganese spins. We stopped the calculation at this level, because convergency tests on the A^α coefficients showed that inclusion of additional spins or chains gave only small variations on the calculated values.

Analysis of the Experimental Relaxation Rates. In the diffusive limit, the nuclear spin–lattice relaxation rates must be frequency dependent,[23] with a $\omega^{-1/2}$ dependence, as we experimentally observe for both ^{19}F and ^1H nuclei. The nuclei here act as probes of the electron correlation, and as a consequence the frequency behavior is independent of the particular nucleus that is employed.

The best test of the model we have worked out comes from the analysis of the frequency dependence of the ^{19}F relaxation rates measured on single crystals with $\theta = 0°$, as shown in Figure 4. The dipolar coefficients can be calculated and $\chi(0)$ is experimentally known; therefore, the only parameter to be fitted in (9) is the diffusion coefficient, D. The best fit diffusion coefficient in this case is $D = 4.6 \times 10^{14}$ rad s^{-1}, which compares well with that expected on a theoretical basis of 1.33×10^{14} rad s^{-1}. Similar differences between expected values and those obtained from the analysis of experimental data have been reported before,[24] and they essentially reflect the simplifications that have been introduced in the theoretical model. However, the prediction of the right order of magnitude for D can be considered as fully satisfactory.

The angular dependence of the relaxation rate was qualitatively reproduced, as shown in Figure 3 for two different frequencies. In this case, we used the spin diffusion coefficient D obtained from the fit of the polycrystalline powder data, so that the calculated angular dependence has no adjustable parameter. All these data confirm the one-dimensional nature of $Mn(hfac)_2(NITiPr)$, and show how it is possible to extend to ferrimagnets the treatment previously used for one-dimensional ferromagnets and antiferromagnets.

In order to fit the experimental ^{19}F relaxation rates of polycrystalline powders, we should integrate (9) over all the crystal orientations. A simplified model has been previously used which assumes that crystallites with $\theta = 90°$ are largely dominant, because the probability of a given orientation goes as $\sin^2\theta$. Therefore, the relaxation rates are calculated for one angular value, reasonably close to 90°. The best fit of the experimental relaxation rates, reported in Figure 2, yields $D = 3.6 \times 10^{15}$ rad s^{-1} for $\theta = 90°$, and $D = 1.9 \times 10^{15}$ rad s^{-1} for $\theta = 60°$, which is slightly larger than the expected value. The same calculation was repeated for the protons, and the results are reported in Figure 2. Since the positions of the hydrogen nuclei were estimated with a large uncertainty, the D value obtained from the fit is less significant.

At low frequencies, both nuclei show a dramatic deviation from diffusive behavior. This is expected, because at very long times both intrachain dipolar interactions and interchain exchange can provide an effective cutoff to the spin correlation; i.e., they provide a pathway for the two-spin correlation functions to go rapidly to zero. In principle also rotation effects of CF_3 or CH_3 groups might cause reversals of the frequency dependence of the relaxation rates, but they would be expected to occur at very different frequencies for the two different groups, while the deviation from diffusive behavior is observed at ca. 20 MHz for both ^{19}F and ^1H.

The cutoff condition can be met on decreasing frequency either when it is the nuclear ω_n or the electron Larmor frequency ω_e that becomes smaller than ω_c. Which is the effective case depends essentially on how large the interactions causing the cutoff are and on the relative values of the electron–nucleus coupling coefficients A^+ and A^z of (7).

In $Mn(hfac)_2(NITiPr)$, the ^{19}F T_1^{-1} data in the high-frequency range down to about 20 MHz are quantitatively well interpreted by using the contribution of both terms in (7), indicating that in this range ω_n is still larger than ω_c, and that the maxima in the relaxation rates on decreasing frequency occur when the condition $\omega_n = \omega_c$ holds.

The cutoff frequency ω_c is related to the largest interaction responsible of the deviations from one-dimensional diffusive behavior. The intrachain dipolar interactions are dominated by the nearest-neighbor manganese–radical interactions. If we assume that the cutoff is determined by these intrachain dipolar interactions, the cutoff frequency is expressed as[24,27]

$$\omega_c = (4D\omega_e)^{-1/2}[F_1^2(\theta) + \sqrt{2}F_2^2(\theta)] \quad (10)$$

where

(48) Bertini, I.; Luchinat, C. *NMR of Paramagnetic Molecules in Biological Systems*; Benjamin Cummings: Menlo Park, CA, 1985.
(49) Caneschi, A.; Gatteschi, D.; Grand, A.; Laugier, J.; Pardi, L.; Rey, P. *Inorg. Chem.* **1988**, *27*, 1031.

$$F_1^2(\theta) = \tfrac{3}{2}[S_{Mn}(S_{Mn}+1)S_{Rad}(S_{Rad}+1)]^{1/2}\sin^2\theta\cos^2\theta\,(\omega_d^2V^2)$$

$$F_2^2(\theta) = \tfrac{3}{4}[S_{Mn}(S_{Mn}+1)S_{Rad}(S_{Rad}+1)]^{1/2}\sin^4\theta\,(\omega_d^2V^2)$$

$$\omega_d = \frac{\hbar\gamma_e^2}{C^3} \qquad V = \Sigma_{ij}\left|\frac{C}{r_{ij}}\right|^3$$

C is the distance between manganese(II) and radical spins in the hypothesis of point dipole (C = 2.82 Å), and V has been calculated for simplicity in the case of a perfectly straight chain.

(10) shows that ω_c is angular dependent; therefore, close insight of the cutoff mechanism would be obtained from the oriented spin-lattice relaxation rates in the low-frequency range. Unfortunately, the small size of the crystals and the reduced NMR spectrometer sensitivity at low frequencies prevented us from exploring the low-frequency range for the oriented crystals. Nevertheless, also from the powders we can get useful information calculating the cutoff frequency assuming that it is dominated by the crystallites with $\theta = 90°$. In this way, we calculate $\nu_c = \omega_c/2\pi \cong 19$ MHz by using the theoretical $D = 1.16\omega_{ex}$ value, while we calculate $\nu_c \cong 15$ MHz by using the D value obtained from the fitting of the single-crystal data, in good agreement with the experimental values ($\nu_c \cong 17$ MHz for ^{1}H and 22 MHz for ^{19}F). The decrease of T_1^{-1} at low frequency is the consequence of the fact that ω_c is frequency dependent with a $\omega^{-1/2}$ law, and of the large contribution of the $A^2j(\omega_n)$ term to the relaxation rate.

The calculations indicate that the cutoff effects can be satisfactorily justified by the dipolar interactions between spins of the same chain. This result is very important because it puts an upper limit on the value of the interchain exchange interaction to $J' \cong 6 \times 10^{-4}$ cm^{-1}. The J'/J ratio is so much smaller than 2×10^{-6}, which confirms the exceptionally good one-dimensional nature of Mn(hfac)$_2$(NITiPr).

Conclusions

In this paper, we have shown how NMR is a powerful tool for the analysis of the magnetic properties of one-dimensional magnetic materials. Theory had already been tested on ferromagnets and antiferromagnets,[24-28] but this is the first example of the successful analysis of a one-dimensional ferrimagnet. In particular, we have confirmed that in Mn(hfac)$_2$(NITiPr) the interchain exchange interactions are exceedingly small, therefore supporting our analysis of the mechanism of transition to three-dimensional order driven by dipolar interactions. The NMR data confirm that at high temperature Mn(hfac)$_2$(NITiPr) is a textbook example of a one-dimensional ferrimagnet as was already suggested on the basis of the EPR spectra.

The numerous one-dimensional magnetic materials that have been recently synthesized by using a molecular approach may be usefully tested with NMR experiments in order to better understand their magnetic properties. Further these materials with many chemically not equivalent protons might also provide the opportunity to observe more than one signal per nucleus, thus providing more refined testing grounds for the theories of spin dynamics in one-dimensional materials. Finally the experiments may be performed also in the vicinity of the transition temperature to three-dimensional magnetic order to obtain insight into the critical fluctuations and the field dependence of the critical temperatures. We are currently working along these lines.

Acknowledgment. Thanks are due to Professor A. Rigamonti, University of Pavia, for constant help in the interpretation of the magnetic data. Stimulating discussions with Professors I. Bertini, University of Florence, and C. Luchinat, University of Bologna, are gratefully acknowledged. The financial support of MURST and of the "Progetto Finalizzato Materiali Speciali per Tecnologie Avanzate" is gratefully acknowledged.

Artificial Manipulation of Apparent Bond Lengths As Determined by Single-Crystal X-ray Diffraction

Keum Yoon and Gerard Parkin*

Contribution from the Department of Chemistry, Columbia University, New York, New York 10027. *Received April 17, 1991*

Abstract: Single crystals composed of solid solutions of pairs of the complexes $\{\eta^3$-HB(3-Bu^{t}pz)$_3\}$ZnCl, $\{\eta^3$-HB(3-Bu^{t}pz)$_3\}$ZnI, and $\{\eta^3$-HB(3-Bu^{t}pz)$_3\}$ZnCH$_3$ [3-Bu^{t}pz = 3-$C_3N_2H_2$Bu^t], over a range of compositions, have been examined by X-ray diffraction. In each case the presence of the impurity is manifested by the observation of an apparent Zn-X bond length that is intermediate between the two possible extremes for the pair of complexes involved. As expected the relationship between the apparent bond length and composition is not linear but is weighted by the relative scattering powers of the disordered groups.

Single-crystal X-ray diffraction is the most widely used technique for the determination of both (i) molecular structures and (ii) accurate bond lengths of complexes in the solid state. However, the occurrence of crystallographic disorder derived from packing identical molecules in different, though structurally similar, orientations may result in the incorrect determination of not only bond lengths but also molecular structures. For example, the molecular structure of the ethylidyne complex W(PMe$_3$)$_4$(CH$_3$)(CCH$_3$) was originally incorrectly assigned as the *dimethyl* derivative W(PMe$_3$)$_4$(CH$_3$)$_2$, as a result of disorder between the ethylidyne and methyl ligands.[1] Disorder of groups that have similar steric requirements (e.g., pairs of atoms) is more common, as illustrated by the example of $\{\eta^3$-HB(pz)$_3\}$Mo(O)Cl$_2$, which shows three different Mo-X bond lengths that are intermediate between Mo=O and Mo-Cl, with none representing either a pure Mo=O or Mo-Cl bond length.[2] A second type of disorder occurs when a *nonidentical*, but structurally related, molecule occupies sites in the crystal lattice. However, even though cocrystallization of isostructural molecules is well-established,[3] the extent of this phenomenon does not appear to be widely appreciated, in part

(1) (a) Jones, R. A.; Wilkinson, G.; Galas, A. M. R.; Hursthouse, M. B. *J. Chem. Soc., Chem. Commun.* **1979**, 926-927. (b) Chiu, K. W.; Jones, R. A.; Wilkinson, G.; Galas, A. M. R.; Hursthouse, M. B.; Malik, K. M. A. *J. Chem. Soc., Dalton Trans.* **1981**, 1204-1211.

(2) Lincoln, S.; Koch, S. A. *Inorg. Chem.* **1986**, *25*, 1594-1602.

(3) For example, doping of paramagnetic materials into crystals of isostructural diamagentic complexes is used exclusively in single-crystal EPR strudies. See, for example: (a) Peterson, J. L.; Dahl, L. F. *J. Am. Chem. Soc.* **1975**, *97*, 6416-6422. (b) Petersen, J. L.; Dahl, L. F. *J. Am. Chem. Soc.* **1975**, *97*, 6422-6433.

0002-7863/91/1513-8414$02.50/0